ELSEVIER

Journal of Biomechanics 35 (2002) 1399–1403

JOURNAL OF BIOMECHANICS

www.elsevier.com/locate/jbiomech
www.JBiomech.com

Technical note

Two-dimensional viscous flow between slowly expanding or contracting walls with weak permeability

Joseph Majdalani[a,*], Chong Zhou[a], Christopher A. Dawson[b]

[a] *Department of Mechanical and Industrial Engineering, Marquette University, 1515 W Wisconsin Avenue, Milwaukee, WI 53233, USA*
[b] *Department of Physiology, Medical College of Wisconsin, Zablocki V.A. Medical Center, Milwaukee, WI 53295-1000, USA*

Accepted 26 June 2002

Abstract

Since the transport of biological fluids through contracting or expanding vessels is characterized by low seepage Reynolds numbers, the current study focuses on the viscous flow driven by small wall contractions and expansions of two weakly permeable walls. The scope is limited to two-dimensional symmetrical solutions inside a simulated channel with moving porous walls. In seeking an exact solution, similarity transformations are used in both space and time. The problem is first reduced to a nonlinear differential equation that is later solved both numerically and analytically. The analytical procedure is based on double perturbations in the permeation Reynolds number R and the wall expansion ratio α. Results are correlated and compared via variations in R and α. Under the auspices of small $|R|$ and $|\alpha|$, the analytical result constitutes a practical equivalent to the numerical solution. We find that, when suction is coupled with wall contraction, rapid flow turning is precipitated near the wall where the boundary layer is formed. Conversely, when injection is paired with wall expansion, the flow adjacent to the wall is delayed. In this case, the viscous boundary layer thickens as injection or expansion rates are reduced. Furthermore, the pressure drop along the plane of symmetry increases when the rate of contraction is increased and when either the rate of expansion or permeation is reduced. As nonlinearity is retained, our solutions are valid from a large cross-section down to the state of a completely collapsed system.

Keywords: Slit flow; Permeable walls; Small perturbations

1. Introduction

Studies of fluid transport in biological organisms are often concerned with the flow of a particular fluid inside an expanding or contracting vessel with permeable walls. For a valved vessel exhibiting deformable boundaries, alternating wall contractions produce the effect of a physiological pump. The flow behavior inside the lymphatics exhibits a similar character. In such models, circulation is induced by successive contractions of two thin sheets that cause the downstream convection of the sandwiched fluid. Seepage across permeable walls is clearly important to the mass transfer between blood, air and tissue (Chang et al., 1989). Its assessment can serve to better understand the function of biological filters such as kidneys and lungs.

The possibility of emulating peristaltic motion by successive wall contractions and expansions is described by Uchida and Aoki (1977) and Goto and Uchida (1990). Since fluctuating stresses can influence the responsiveness of endothelial cells (Nerem and Levesque, 1987), their accurate determination in a pulsating environment may be appropriate of a number of investigations concerned with the characterization of atherosclerosis (see Dewey et al., 1981; Levesque and Nerem, 1985; Levesque et al., 1989). Considering that abnormalities in fluctuating stresses have been associated with this disease (Sprague et al., 1987), identification of the role of flow dynamics can be meaningful in predicting pulsatory flow attributes. Such results could be used toward a proper characterization of mechanically assisted respiration (Drazen et al., 1984), hemodialysis in artificial kidneys (Wang, 1971) and peristaltic transport (Fung and Yih, 1968).

The viscous flow inside an impermeable tube of contracting cross section was first examined by Uchida

*Corresponding author. Tel.: +1-414-288-6877; fax: +1-414-288-7082.
E-mail address: maji@mu.edu (J. Majdalani).

0021-9290/02/$ - see front matter
PII: S0021-9290(02)00186-0

and Aoki (1977). Therein, the Navier–Stokes equations for a semi-infinite tube were reduced to a single differential equation (Cox and King, 1997). This 'exact' reduction was precipitated by a viable similarity transformation in space and time. Their equation was then solved *numerically* and used to explain the principal flow characteristics. In a later study by Goto and Uchida (1990), the similarity analysis was repeated for a contracting tube with permeable walls.

The first study by Uchida and Aoki (1977) constituted a visible improvement over former studies of peristaltic pumping that considered either inviscid flows (Jones, 1969) or pulsating flows inside infinitely long, valveless tubes (cf. Lighthill, 1972; Jaffrin and Shapiro, 1971; Shapiro et al., 1969; Fung and Yih, 1968). The second study by Goto and Uchida (1990) not only captured the effects of viscosity, wall contraction, and realistic body length, but also accounted for the effect of wall permeability. Their ODE was hence capable of embracing the equations produced by Yuan and Finkelstein (1956), and Terrill and Thomas (1969) for a permeable tube with stationary walls. In principle, results obtained by other investigators could be reproduced from Goto and Uchida's differential equation by setting its wall expansion rate to zero.

Under the assumption of weak permeability and slow wall motion, the current study focuses on obtaining an asymptotic solution for the equivalent slit flow problem. In the process, the reader will be exposed to the complete development of the governing equation in rectilinear coordinates. This will be followed by an asymptotic solution that can be corroborated by numerics. Our planar solution will be carried out without imposing any of the overly simplifying assumptions used in previous studies (e.g. Wang, 1971; Bhatnagar, 1979).

2. Method

Consider the laminar, isothermal, and incompressible flow in a rectangular domain bounded by two permeable surfaces that enable the fluid to enter or exit during successive expansions or contractions. A planar section of the simulated domain is shown in Fig. 1. One side of the cross section, representing the distance ($2a$) between the walls is taken to be smaller than the other two (W and L). Both walls are assumed to have equal permeability and to expand uniformly at a time-dependent rate $\dot{a}$. Furthermore, the origin $\hat{x}=0$ is assumed to be the center of the classic squeeze film problem. This enables us to assume flow symmetry about $\hat{x}=0$. Under these assumptions, the equations for continuity and motion become

$$\frac{\partial \hat{u}}{\partial \hat{x}}+\frac{\partial \hat{v}}{\partial \hat{y}}=0,$$
$$\frac{\partial \hat{u}}{\partial t}+\hat{u}\frac{\partial \hat{u}}{\partial \hat{x}}+\hat{v}\frac{\partial \hat{u}}{\partial \hat{y}}=-\frac{1}{\rho}\frac{\partial \hat{p}}{\partial \hat{x}}+\nu\nabla^2\hat{u},$$
$$\frac{\partial \hat{v}}{\partial t}+\hat{u}\frac{\partial \hat{v}}{\partial \hat{x}}+\hat{v}\frac{\partial \hat{v}}{\partial \hat{y}}=-\frac{1}{\rho}\frac{\partial \hat{p}}{\partial \hat{y}}+\nu\nabla^2\hat{v}, \quad (1)$$

where $\hat{p}$, ρ, ν, and t are the dimensional pressure, density, kinematic viscosity, and time. Auxiliary conditions can be specified such as

$$\hat{u}(\hat{x},a)=0, \quad \hat{v}(a)=-v_w=-\dot{a}/c,$$
$$\frac{\partial \hat{u}}{\partial \hat{y}}(\hat{x},0)=0, \quad \hat{v}(0)=0, \quad \hat{u}(0,\hat{y})=0. \quad (2)$$

The injection or suction coefficient ($c\equiv \dot{a}/v_w$) that appears in Eq. (2) is a measure of wall porosity (Goto and Uchida, 1990). At this point, the stream function and mean flow vorticity can be introduced by putting

$$\hat{u}=\frac{\partial \hat{\psi}}{\partial \hat{y}}, \quad \hat{v}=\frac{\partial \hat{\psi}}{\partial \hat{x}}, \quad \hat{\zeta}=\frac{\partial \hat{v}}{\partial \hat{x}}-\frac{\partial \hat{u}}{\partial \hat{y}},$$
$$\frac{\partial \hat{\zeta}}{\partial t}+\hat{u}\frac{\partial \hat{\zeta}}{\partial \hat{x}}+\hat{v}\frac{\partial \hat{\zeta}}{\partial \hat{y}}=\nu\left[\frac{\partial^2\hat{\zeta}}{\partial \hat{x}^2}+\frac{\partial^2\hat{\zeta}}{\partial \hat{y}^2}\right]. \quad (3)$$

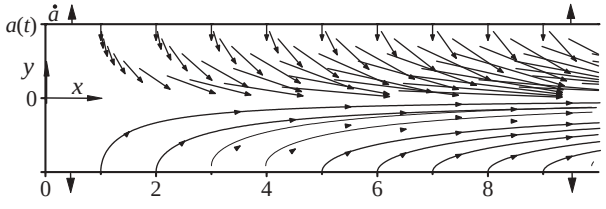

Fig. 1. Two-dimensional domain with expanding or contracting porous walls.

2.1. The Proudman–Johnson equation

Due to mass conservation, a similar solution can be developed with respect to $\hat{x}$. Starting with

$$\hat{\psi}=\nu\hat{x}\hat{F}(y,t)/a, \quad y=\hat{y}/a, \quad \hat{u}=\nu\hat{x}a^{-2}\hat{F}_y,$$
$$\hat{v}=-\nu a^{-1}\hat{F}(y,t), \quad \hat{F}_y\equiv \partial\hat{F}/\partial y, \quad (4)$$

substitution into Eq. (3) yields

$$\hat{u}_{\hat{y}t}+\hat{u}\hat{u}_{\hat{y}\hat{x}}+\hat{v}\hat{u}_{\hat{y}\hat{y}}=\nu\hat{u}_{\hat{y}\hat{y}\hat{y}}. \quad (5)$$

In order to solve Eq. (5), one uses the chain rule to obtain

$$\hat{F}_{yyyy}+\alpha(y\hat{F}_{yyy}+3\hat{F}_{yy})+\hat{F}\hat{F}_{yyy}-\hat{F}_y\hat{F}_{yy}$$
$$-a^2\nu^{-1}\hat{F}_{yyt}=0, \quad (6)$$

where $\alpha(t)\equiv \dot{a}a/\nu$ is the nondimensional wall dilation rate defined positive for expansion. Note that Eq. (6) is a generalization of the Proudman–Johnson equation obtained by retaining the effect of wall motion (Proudman and Johnson, 1962). A careful integration of

Eq. (6) produces

$$\hat{F}_{yyy} + \alpha(y\hat{F}_{yy} + 2\hat{F}_y) + \hat{F}\hat{F}_{yy} - (\hat{F}_y)^2 - a^2 v^{-1}\hat{F}_{yt} = \lambda, \quad \lambda \neq \lambda(y). \tag{7}$$

Boundary conditions given by Eq. (2) translate into

$$\hat{F}_{yy}(0) = 0, \quad \hat{F}(0) = 0, \quad \hat{F}_y(1) = 0, \quad \hat{F}(1) = R, \tag{8}$$

where R is the permeation Reynolds number defined by $R \equiv av_w/v > 0$ for injection. This number happens to be a small quantity in many biological applications (Fung and Yih, 1968; Womersley, 1955). A similar solution with respect to time can also be obtained following the same lines described by Uchida and Aoki (1977). This can be accomplished by considering the case for which the nondimensional parameter $\alpha(t) \equiv \dot{a}_0 a_0/v$ remains constant.

2.2. Dimensionless set

Eqs. (4), (6) and (8) can be normalized by putting

$$\psi = \frac{\hat{\psi}}{a\dot{a}}, \quad u = \frac{\hat{u}}{\dot{a}}, \quad v = \frac{\hat{v}}{\dot{a}}, \quad x = \frac{\hat{x}}{a}, \quad F = \frac{\hat{F}}{R} \tag{9}$$

and so

$$\psi = xF/c, \quad u = xF'/c, \quad v = -F/c, \quad c = \alpha/R, \tag{10}$$

$$F^{IV} + \alpha(yF''' + 3F'') + RFF''' - RF'F'' = 0, \tag{11}$$

$$F''(0) = 0, \quad F(0) = 0, \quad F'(1) = 0, \quad F(1) = 1, \tag{12}$$

where a prime denotes differentiation with respect to y. Note that Berman's well-known ODE (Berman, 1953) can be viewed as a special case of Eq. (11) with $\alpha = 0$.

3. Results

For small injection and suction, one may use R as a perturbation parameter and expand the solution in a series of diminishing terms by substituting $F = F_0 + RF_1 + O(R^2)$ into Eq. (11). The leading order equation becomes

$$F_0^{IV} + \alpha(yF_0''' + 3F_0) = 0;$$
$$F_0''(0) = 0, \quad F_0(0) = 0, \quad F_0'(1) = 0, \quad F_0(1) = 1. \tag{13}$$

In like fashion, the first order equation and boundary conditions can be segregated into

$$F_1^{IV} + \alpha(yF_1''' + 3F_1) = F_0'F_0'' - F_0F_0''';$$
$$F_1''(0) = 0, \quad F_1(0) = 0, \quad F_1'(1) = 0, \quad F_1(1) = 0. \tag{14}$$

Since α is also small, it can be used as a secondary perturbation parameter. To proceed, one lets

$$F_0 = F_{00} + \alpha F_{01} + O(\alpha^2). \tag{15}$$

Forthwith, two sets of equations emerge at leading and first orders in α. These are

$$F_{00}^{IV} = 0; \quad F_{00}''(0) = 0, \quad F_{00}(0) = 0,$$
$$F_{00}'(1) = 0, \quad F_{00}(1) = 1 \tag{16}$$

and

$$F_{01}^{IV} + yF_{00}''' + 3F_{00} = 0;$$
$$F_{01}''(0) = 0, \quad F_{01}(0) = 0, \quad F_{01}'(1) = 0, \quad F_{01}(1) = 0. \tag{17}$$

The first group yields

$$F_{00} = -\tfrac{1}{2}y^3 + \tfrac{3}{2}y, \quad F_{01}^{IV} = \tfrac{3}{2}y^3 - \tfrac{3}{2}y. \tag{18}$$

The latter can be readily integrated while fulfilling the boundary condition in Eq. (17). The result is

$$F_{01} = \tfrac{1}{560}y^7 - \tfrac{1}{80}y^5 + \tfrac{11}{560}y^3 - \tfrac{1}{112}y. \tag{19}$$

Combining F_{00} and F_{01}, the leading order solution becomes

$$F_0 = -\tfrac{1}{2}y^3 + \tfrac{3}{2}y + \alpha(\tfrac{1}{560}y^7 - \tfrac{1}{80}y^5 + \tfrac{11}{560}y^3 - \tfrac{1}{112}y). \tag{20}$$

To evaluate F_1, this process is repeated. We start by substituting Eq. (20) into Eq. (14) and find

$$\begin{aligned} F_1^{IV} &+ \alpha(yF_1''' + 3F_1) \\ &= [-\tfrac{3}{2}y^2 + \tfrac{3}{2} + \alpha(\tfrac{1}{80}y^6 - \tfrac{1}{16}y^4 + \tfrac{33}{560}y^2 - \tfrac{1}{112})] \\ &\times [-3y + \alpha(\tfrac{3}{40}y^5 - \tfrac{1}{4}y^3 + \tfrac{33}{280}y)] \\ &- [-\tfrac{1}{2}y^3 + \tfrac{3}{2}y + \alpha(\tfrac{1}{560}y^7 - \tfrac{1}{80}y^5 + \tfrac{11}{560}y^3 - \tfrac{1}{112}y)] \\ &\times [-3 + \alpha(\tfrac{3}{8}y^4 - \tfrac{3}{4}y^2 + \tfrac{33}{280})]. \end{aligned} \tag{21}$$

Again, we use α as our secondary perturbation parameter and let $F_1 = F_{10} + \alpha F_{11} + O(\alpha^2)$. Collecting terms of the same order in α yields

$$F_{10}^{IV} = 3y^3; \quad F_{10}''(0) = 0, \quad F_{10}(0) = 0,$$
$$F_{10}'(1) = 0, \quad F_{10}(1) = 0, \tag{22}$$

$$F_{10} = \tfrac{1}{280}y^7 - \tfrac{3}{280}y^3 + \tfrac{1}{140}y. \tag{23}$$

Next, we consider

$$F_{11}^{IV} = \tfrac{3}{70}y^7 - \tfrac{3}{2}y^5 + \tfrac{18}{35}y^3 + \tfrac{9}{35}y;$$
$$F_{11}''(0) = 0, \quad F_{11}(0) = 0, \quad F_{11}'(1) = 0, \quad F_{11}(1) = 0, \tag{24}$$

$$\begin{aligned} F_{11} = &\tfrac{1}{184800}y^{11} - \tfrac{1}{2016}y^9 + \tfrac{3}{4900}y^7 + \tfrac{3}{1400}y^5 \\ &- \tfrac{3233}{776160}y^3 + \tfrac{2459}{1293600}y. \end{aligned} \tag{25}$$

At length, the complete solution for Eq. (11) can be put into

$$\begin{aligned} F = &-\tfrac{1}{2}y^3 + \tfrac{3}{2}y + \alpha(\tfrac{1}{560}y^7 - \tfrac{1}{80}y^5 + \tfrac{11}{560}y^3 + \tfrac{1}{112}y) \\ &+ R[\tfrac{1}{280}y^7 - \tfrac{3}{280}y^3 + \tfrac{1}{140}y + \alpha(\tfrac{1}{184800}y^{11} - \tfrac{1}{2016}y^9 \\ &+ \tfrac{3}{4900}y^7 + \tfrac{3}{1400}y^5 - \tfrac{3233}{776160}y^3 + \tfrac{2459}{1293600}y)]. \end{aligned} \tag{26}$$

At this juncture, it may be useful to note that, by suppressing the motion of the wall (for $\alpha = 0$), the small R solution given by Berman (1953) is recovered from Eq. (26). To evaluate the principal flow variables, some

of the derivatives of F are needed. These are

$$F' = -\tfrac{3}{2}y^2 + \tfrac{3}{2} + \alpha(\tfrac{1}{80}y^6 - \tfrac{1}{16}y^4 + \tfrac{33}{560}y^2 - \tfrac{1}{112}) + R[\tfrac{1}{40}y^6 - \tfrac{9}{280}y^2 + \tfrac{1}{140} + \alpha(\tfrac{1}{16800}y^{10} - \tfrac{1}{224}y^8 + \tfrac{3}{700}y^6 + \tfrac{3}{280}y^4 - \tfrac{3233}{258720}y^2 + \tfrac{2459}{1293600})], \quad (27)$$

$$F'' = -3y + \alpha(\tfrac{3}{20}y^5 - \tfrac{1}{4}y^3 + \tfrac{33}{280}y) + R[\tfrac{3}{20}y^5 - \tfrac{9}{140}y + \alpha(\tfrac{1}{1680}y^9 - \tfrac{1}{28}y^7 + \tfrac{9}{350}y^5 + \tfrac{3}{70}y^3 - \tfrac{3233}{129360}y)], \quad (28)$$

$$F''' = -3 + \alpha(\tfrac{3}{8}y^4 - \tfrac{3}{4}y^2 + \tfrac{33}{280}) + R[\tfrac{3}{4}y^4 - \tfrac{9}{140} + \alpha(\tfrac{3}{560}y^8 - \tfrac{1}{4}y^6 + \tfrac{9}{70}y^4 + \tfrac{9}{70}y^2 - \tfrac{3233}{129360})]. \quad (29)$$

4. Discussion

From the characteristic function F, all flow variables can be determined either asymptotically, from the foregoing formulations, or numerically, from a Runge–Kutta solver. Using a constant dilation rate of $\alpha = \pm 0.5$, numerical and analytical solutions for uc/x (or F') are illustrated in Fig. 2. From the graph, it may be realized that Eq. (27) is a fair approximation to the numerical solution for $-5 \leqslant R \leqslant 5$. Furthermore, the largest asymptotic error seems to occur in the vicinity of the core and for relatively larger values of $|R|$. These results are confirmatory because they indicate a consistent improvement in the accuracy of the analytical expressions at lower permeation rates. Since their accuracy is commensurate with the smallness of $|R|$, the analytical expressions become gradually more suitable to model biological seepage across permeable membranes.

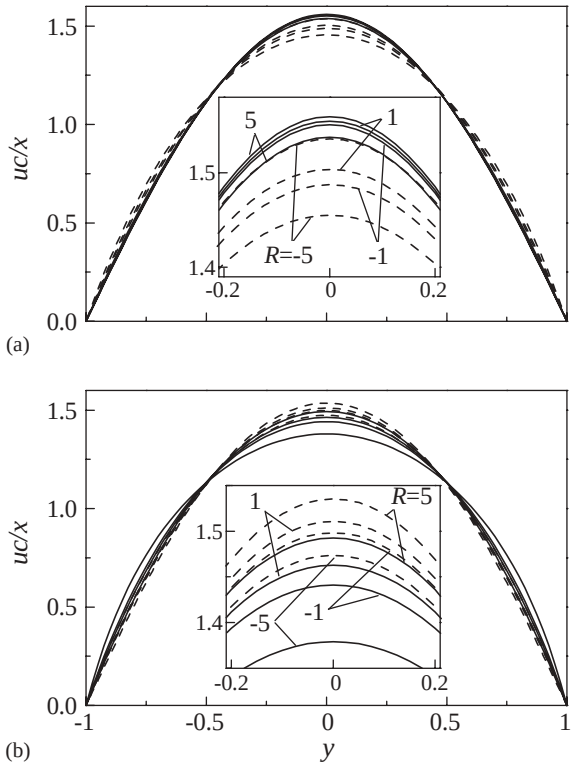

Fig. 2. Comparison between numerical (—) and analytical (- - -) solutions for uc/x at (a) $\alpha = 0.5$ and (b) $\alpha = -0.5$; $-5 \leqslant R \leqslant 5$. Enlargements are shown in the insets. Note that the discrepancy between the numerical and analytical predictions diminishes as the net permeation Reynolds number is reduced.

Having briefly examined the velocity field, the remaining flow properties, such as pressure and stress distributions, can be studied as well. The normal pressure gradient can be obtained by substituting the velocity components into Eq. (1). One obtains

$$p_y = -[R^{-1}F'' + FF' + \alpha R^{-1}(F + yF')],$$
$$p = \hat{p}/(\rho v_w^2). \quad (30)$$

The normal pressure distribution can now be determined by integrating Eq. (30). Letting p_c be the centerline pressure, one may proceed from

$$\int_{p_c}^{p(y)} \mathrm{d}p = \int_0^y -[R^{-1}F'' + FF' + \alpha R^{-1}(F + yF')]\,\mathrm{d}y. \quad (31)$$

Then using $FF' = \frac{1}{2}(F^2)'$, and $(F + yF') = (yF)'$, one integrates Eq. (31) into

$$\Delta p_n = R^{-1}F'(0) - (R^{-1}F' + \tfrac{1}{2}F^2 + \alpha R^{-1}yF). \quad (32)$$

Fig. 3 illustrates the pressure distribution in the normal direction. Comparing Figs. 3a and b, the sensitivity of the pressure to variations in wall expansion appears to be slightly less significant for injection combined with wall contraction (or, conversely, for suction combined with wall expansion). As explained earlier, combining injection (positive R) with wall contraction (negative α) yields a smaller effective Reynolds number. Due to the doubly perturbed nature of the analytical solutions, a smaller error is expected when the secondary perturbation parameter $|\alpha|$ becomes much smaller than the primary parameter $|R|$. This explains the improved precision associated with the analytical solution at smaller values of $|\alpha|$.

Similar substitutions into the axial momentum equation give rise to an expression for the axial pressure gradient. Starting with

$$p_x = x[R^{-1}F''' + FF'' + (F')^2 + \alpha R^{-1}(2F' + yF'')], \quad (33)$$

the axial pressure distribution at any spatial location can be integrated for. One obtains

$$\Delta p_a = \tfrac{1}{2}x^2[R^{-1}F''' + FF'' + (F')^2 + \alpha R^{-1}(2F' + yF'')]. \quad (34)$$

The character of the axial pressure distribution can be studied for both contraction and expansion ($-1 \leqslant \alpha \leqslant 1$) together with suction and injection ($-5 \leqslant R \leqslant 5$). We find that the absolute pressure drop increases as the absolute

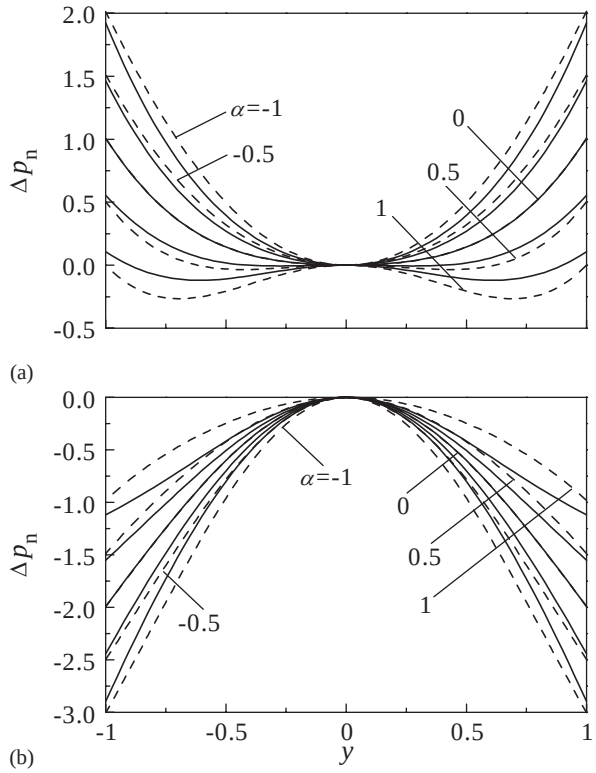

Fig. 3. Comparison between numerical (—) and analytical (- - -) pressure drops in the normal direction for (a) $R = 1$ and (b) $R = -1$; $-1 \leqslant \alpha \leqslant 1$. For every level of injection or suction, the absolute pressure change is largest near the walls. Increasing the speed of the wall also increases the pressure change.

permeation Reynolds number $|R|$ is decreased. Additionally, we find that the higher the contraction velocity is, the greater the pressure drop will be. Hence, the absolute pressure drop increases as α is decreased. Over the specified range of operating parameters, the pressure drop appears to be favorable for injection but can be adverse for suction.

To find the friction force, one may use $\hat{\tau} = \mu(\hat{v}_{\hat{x}} + \hat{u}_{\hat{y}})$ and obtain $\hat{\tau} = \rho v^2 \hat{x} a^{-3} \hat{F}''$ or $\tau = \hat{\tau}/(\rho v_w^2) = R^{-1} x F''$. Clearly, as the Reynolds number is increased, the role of viscosity diminishes, and the shear stress at the wall becomes less significant. Since the normalized shear stress τ_w is inversely proportional to R, the absolute discrepancy between asymptotics and numerics becomes gradually less noticeable with increasing $|R|$.

The analytical approximations provided heretofore compare favorably with numerical solutions over a useful range of parameters. Due to their adequate accuracy, these explicit approximations are practically equivalent to the exact solution for sufficiently small $|R|$ and $|\alpha|$. In view of the small permeation and wall motion, it can be argued that differences between flat and curved walls become small. From that standpoint, the planar solution presented here can be used to approximate the flow inside a thin annulus with permeable walls. As the Navier–Stokes nonlinearity is retained in full, the analytical solutions are valid down to the state of a completely collapsed channel.

References

Berman, A.S., 1953. Laminar flow in channels with porous walls. Journal of Applied Physics 24, 1232–1235.

Bhatnagar, R.K., 1979. Fluctuating flow of a viscoelastic fluid in a porous channel. Transactions of the ASME: Journal of Applied Mechanics 46, 21–25.

Chang, H.N., Ha, J.S., Park, J.K., Kim, I.H., Shin, H.D., 1989. Velocity field of pulsatile flow in a porous tube. Journal of Biomechanics 22, 1257–1262.

Cox, S.M., King, A.C., 1997. On the asymptotic solution of a high-order nonlinear ordinary differential equation. Proceedings of the Royal Society of London, Series A 453, 711–728.

Dewey, C.F.J., Bussolari, S.R., Gimbrone, M.A.J., Davis, P.F., 1981. The dynamic response of vascular endothelial cells to fluid shear stress. Journal of Biomechanical Engineering 103, 177.

Drazen, J.M., Kamm, R.D., Slutsky, A.S., 1984. High frequency ventilation. Physiological Reviews 64, 505–543.

Fung, Y.C., Yih, C.S., 1968. Peristaltic transport. Journal of Applied Mechanics 35, 669–675.

Goto, M., Uchida, S., 1990. Unsteady flow in a semi-infinite contracting or expanding pipe with a porous wall. In: Proceedings of the 40th Japan National Congress Applied Mechanics NCTAM-40, Japan National Congress for Applied Mechanics, Tokyo, Japan, pp. 163–172.

Jaffrin, M.Y., Shapiro, A.H., 1971. Peristaltic pumping. Annual Review of Fluid Mechanics 3, 13–36.

Jones, R.T., 1969. Blood flow. Annual Review of Fluid Mechanics 1, 223–244.

Levesque, M.J., Nerem, R.M., 1985. Elongation and orientation of cultured endothelial cells in response to shear. Journal of Biomechanical Engineering., 341–347.

Levesque, M.J., Sprague, E.A., Schwartz, C.J., Nerem, R.M., 1989. The influence of shear stress on cultured vascular endothelial cells: the stress response of an anchorage-dependent mammalian cell. Biotechnical Progress 5, 1–8.

Lighthill, M.J., 1972. Physiological fluid dynamics: a survey. Journal of Fluid Mechanics A 52, 475–497.

Nerem, R.M., Levesque, M.J., 1987. Hemodynamics and the arterial wall. Vascular Diseases, 295–317.

Proudman, I., Johnson, K., 1962. Boundary-layer growth near a rear stagnation point. Journal of Fluid Mechanics 12, 161–168.

Shapiro, A.H., Jaffrin, M.Y., Weinberg, S.L., 1969. Peristaltic pumping with long wavelengths at low Reynolds number. Journal of Fluid Mechanics 37, 799–825.

Sprague, E.A., Steinbach, B.L., Nerem, R.M., Schwartz, C.J., 1987. Influence of a laminar steady state fluid-imposed wall shear stress on the binding internalization, and degradation of low density lipoproteins by cultured arterial endothelium. Circulation 76, 648–656.

Terrill, R.M., Thomas, P.W., 1969. On laminar flow through a uniformly porous pipe. Applied Science Research 21, 37–67.

Uchida, S., Aoki, H., 1977. Unsteady flows in a semi-infinite contracting or expanding pipe. Journal of Fluid Mechanics 82, 371–387.

Wang, C.Y., 1971. Pulsatile flow in a porous channel. Transactions of the ASME: Journal of Applied Mechanics 38, 553–555.

Womersley, J.R., 1955. Method for the calculation of velocity, rate of flow and viscous drag in arteries when the pressure gradient is known. Journal of Physiology 127, 553–563.

Yuan, S.W., Finkelstein, A.B., 1956. Laminar pipe flow with injection and suction through a porous wall. Transactions of the ASME: Journal of Applied Mechanics E 78, 719–724.